JOINT HOT AND COLD CLUTTER MITIGATION IN THE TRANSMIT BEAMSPACE-BASED MIMO RADAR

Yongzhe Li[†‡], *Sergiy A. Vorobyov*[‡], *and Zishu He*[†]

[†]Dept. EE, University of Electronic Science and Technology of China, Chengdu, 611731, China
[‡]Dept. Signal Processing and Acoustics, Aalto University, P.O. Box 13000, FI-00076 Aalto, Finland
Emails: lyzlyz888@gmail.com/yongzhe.li@aalto.fi, svor@ieee.org, zshe@uestc.edu.cn

ABSTRACT

In this paper, the problem of joint hot and cold clutter mitigation in the context of transmit beamspace (TB)-based multiple-input multiple-output (MIMO) radar is studied. The TB-based MIMO radar enables special spatio-temporal structure and low rank of clutter covariance matrices. To efficiently mitigate the hot clutter such as terrain scattered multipath jamming concentrated in the sector-of-interest and the enhanced cold clutter due to transmit energy focusing, we resort to three-dimensional (3D) space-time adaptive processing (STAP) technique. A new 3D STAP method is proposed, which significantly reduces the computational complexity. We show from interference mitigation perspective that the TB-based MIMO radar enables superior output signal-to-interference-plus-noise ratio to that of its traditional MIMO radar counterpart.

***Index Terms*—**Colocated MIMO radar, joint clutter mitigation, space-time adaptive processing (STAP), transmit beamspace (TB).

1. INTRODUCTION

The multiple-input multiple-output (MIMO) radar has become a research field of significant interest in recent years [1]–[15]. Transmit beamforming techniques have been employed to achieve desired beampattern (possibly flat) that covers a certain spatial sector of interest (SOI) [5]–[10]. Additional benefit in terms of signal-to-noise ratio (SNR) gain can be obtained if much less number of waveforms than that employed in the traditional MIMO radar are used [8], i.e., transmit coherent processing gain [7] and waveform diversity [1] are jointly achieved. Superior direction-of-arrival estimation performance, for example, can be achieved in the presence of only noise due to this core feature [8], [10]. Moreover, flexible correlated waveforms are also allowed to be emitted [13]. Such advantages motivate us to further investigate the question on how the transmit beamspace (TB)-based MIMO radar behaves in the environment when both interference and noise are present. The situation of special interest is when hot clutter [16] and cold clutter [17] are both present simultaneously. Cold clutter energy is concentrated within the SOI, and terrain scattered multipath or diffuse jamming that represents the hot clutter occupying the whole SOI can further have a significant impact on the performance of the TB-based MIMO radar. Different from the clutter mitigation in the phased-array (PA) radar [18]–[22], the TB-based MIMO radar enables special spatio-temporal structure and low rank of clutter covariance matrices due to its TB strategy [8], [10]. To the best of our knowledge, the potential of the TB-based MIMO radar on joint clutter mitigation has not been studied previously.

In this paper, we aim at studying and verifying benefits of the TB-based MIMO radar from the perspective of clutter mitigation. Motionless hot clutter such as terrain scattered multipath or diffuse jamming together with ground reflected cold clutter are both involved in the interference environment. We resort to three-dimensional (3D) space-time adaptive processing (STAP) technique to achieve the mitigation goal. Utilizing the special spatio-temporal structure produced by the TB strategy as well as the low-rank and block diagonal hot and cold clutter covariance matrices, we propose a new 3D STAP method with low computational complexity. Passive receiving and off-line clutter subspace calculation with respect to (w.r.t.) radar geometry are used in this method. We show that the TB-based MIMO radar enables superior output signal-to-interference-plus-noise ratio (SINR) to that of its traditional MIMO radar counterpart under efficient clutter mitigation.

2. SIGNAL MODEL

Consider an airborne colocated MIMO radar system with a transmit array of M antenna elements and a receive array of N antenna elements. Both arrays are assumed to be closely located, therefore, they share an identical spatial angle for a far-field target. In the context of the TB-based MIMO radar, K (in general, $K \leq M$) initially orthogonal waveforms are transmitted via K synthesized transmit beams [8]. Let $\boldsymbol{\phi}(t) = [\phi_1(t), \ldots, \phi_K(t)]^T$ be the $K \times 1$ vector of the transmitted waveform values for a given fast time t where $(\cdot)^T$ stands for the transpose operation. We assume that the transmitted waveforms are orthogonal to each other over the time interval of radar pulse duration T_p. The signal radiated towards the spatial direction θ through the kth transmit beam can be

Y. Li's work is supported by China Scholarship Council (CSC).

modeled as [8]

$$s_k(t) = \sqrt{\frac{E}{K}}\big(\mathbf{c}_k^H \mathbf{a}(\theta)\big)\phi_k(t),\ k = 1, \ldots, K \tag{1}$$

where E is the total transmit energy, $\mathbf{a}(\theta)$ is the transmit antenna array steering vector, $\mathbf{c}_k$ is the kth unit-norm column vector of the $M \times K$ TB matrix $\mathbf{C}$ which is defined as $\mathbf{C} \triangleq [\mathbf{c}_1, \ldots, \mathbf{c}_K]$, and $(\cdot)^H$ stands for the Hermitian transpose. From the elementspace perspective, one of the possible transmit schemes is to individually emit the following compound waveforms by the M transmit antenna elements [23]

$$\tilde{s}_m(t) = \sqrt{\frac{E}{K}} \sum_{k=1}^{K} c_k^m \phi_k(t),\ m = 1, \ldots, M \tag{2}$$

where c_k^m is the mth element of $\mathbf{c}_k$.

Let us assume that one radar coherent processing interval (CPI) contains L pulses, and the ground range (ring) of interest (ROI) is separated into N_c ($N_c \gg KNL$) patches. The number of J independent motionless jammers is present, and the jamming signal (to be specific, barrage noise) generated by each hostile jammer is propagated through P independent propagation paths which generally include the direct, specular, and diffuse ones. Thus, in the presence of the target and for the τth pulse , the $N \times 1$ complex vector of array observations from the ROI can be expressed as

$$\begin{aligned}\mathbf{x}(t,\tau) = &\sqrt{\frac{E}{K}}\alpha_{\mathrm{t}} D_{\mathrm{t}}(\tau)\Big(\big(\mathbf{C}^H\mathbf{a}(\theta_{\mathrm{t}})\big)^T \boldsymbol{\phi}(t-\zeta_0)\Big)\mathbf{b}(\theta_{\mathrm{t}})\\ &+\sqrt{\frac{E}{K}}\sum_{i=1}^{N_c}\xi_i D_i(\tau)\Big(\big(\mathbf{C}^H\mathbf{a}(\theta_i)\big)^T \boldsymbol{\phi}(t-\zeta_0)\Big)\mathbf{b}(\theta_i)\\ &+\sum_{j=1}^{J}\sum_{p=1}^{P}\beta_j^p s_j^p(t-\zeta_0,\tau)\mathbf{b}\big(\vartheta_j^p\big) + \mathbf{z}(t,\tau)\end{aligned} \tag{3}$$

where t and τ are respectively the fast- and slow-time indices, ζ_0 is the fast-time delay of the ROI, θ_{t}, θ_i, and ϑ_j^p are spatial angles of the target, the ith clutter patch, and the pth scatter associated with the jth jamming source, respectively, α_{t}, ξ_i, and β_j^p are the complex reflection coefficients of the target, the ith clutter patch, and the jth jamming source associated with the pth propagation path with variances σ_α^2, $\sigma_{\xi_i}^2$, and $\sigma_{\beta_{j,p}}^2$, respectively, $D_{\mathrm{t}}(\tau)$ and $D_i(\tau)$ are respectively the Doppler shifts of the target and the ith clutter patch introduced by the relative motions w.r.t. the radar platform, $s_j^p(t,\tau)$ is the jth jamming signal through the pth propagation path (i.e., a time delayed version of the jth original jamming signal) at the fast-time index t and the slow-time index τ, $\mathbf{b}(\theta)$ is the receive antenna array steering vector, and $\mathbf{z}(t,\tau)$ is the $N \times 1$ white Gaussian noise term.

By match filtering the receive data $\mathbf{x}(t,\tau)$ to the K original orthogonal waveforms at the fast-time index ζ (matched filtering of the ROI occurs at ζ_0) and stacking the filtered outputs for all slow-time pulses, the $LKN \times 1$ virtual data vector can be obtained as

$$\begin{aligned}\mathbf{y}(\zeta) &= \mathrm{vec}\Big(\textstyle\int_{T_p}\mathbf{x}(t,\tau)\boldsymbol{\phi}^H(t-\zeta)\mathrm{d}t\Big)_{\tau=1,\ldots,L}\\ &= \sqrt{\frac{E}{K}}\alpha_{\mathrm{t}}\mathbf{d}(\theta_{\mathrm{t}})\otimes\mathbf{u}(\theta_{\mathrm{t}},\zeta)\otimes\mathbf{b}(\theta_{\mathrm{t}})\\ &\quad+\sqrt{\frac{E}{K}}\sum_{i=1}^{N_c}\xi_i\mathbf{d}(\theta_i)\otimes\mathbf{u}(\theta_i,\zeta)\otimes\mathbf{b}(\theta_i)\\ &\quad+\sum_{j=1}^{J}\sum_{p=1}^{P}\beta_j^p\boldsymbol{\eta}_j^p(\zeta)\otimes\mathbf{b}\big(\vartheta_j^p\big)+\tilde{\mathbf{z}}(\zeta) \qquad (4)\\ &\triangleq \mathbf{y}_{\mathrm{t}}(\zeta)+\mathbf{y}_c(\zeta)+\mathbf{y}_h(\zeta)+\tilde{\mathbf{z}}(\zeta) \qquad (5)\end{aligned}$$

where $\mathbf{u}(\theta,\zeta) \triangleq \mathbf{R}_{\boldsymbol{\phi}}^T(\zeta)\big(\mathbf{C}^H\mathbf{a}(\theta)\big)$ with $\mathbf{R}_{\boldsymbol{\phi}}(\zeta)$ being defined as $\mathbf{R}_{\boldsymbol{\phi}}(\zeta) \triangleq \int_{T_p}\boldsymbol{\phi}(t)\ \boldsymbol{\phi}^H(t-\zeta+\zeta_0)\mathrm{d}t$, $\mathbf{d}(\theta)$ is the Doppler steering vector, $\boldsymbol{\eta}_j^p(\zeta)$ is a $KL \times 1$ vector associated with the pth propagation of the jth jamming signal with its τth $K \times 1$ component being defined as $\boldsymbol{\eta}_j^p(\zeta,\tau) \triangleq \int_{T_p} s_j^p(t-\zeta_0,\tau)\boldsymbol{\phi}^H(t-\zeta)\mathrm{d}t$, $\tilde{\mathbf{z}}(\zeta)$ is the stacked noise term whose covariance is denoted by $\sigma_z^2\mathbf{I}_{LKN}$ with $\mathbf{I}_{LKN}$ being the identity matrix of size $LKN \times LKN$, $\mathrm{vec}(\cdot)$ is the operator that stacks the columns of a matrix into one column vector, and $\otimes$ denotes the Kronecker product. Note that $\mathbf{y}_{\mathrm{t}}(\zeta)$, $\mathbf{y}_c(\zeta)$, and $\mathbf{y}_h(\zeta)$ are used in (5) to denote the space-(slow) time virtual data vectors of the target, the cold clutter, and the hot clutter filtered at the fast-time index ζ, respectively, and they are assumed to be not correlated with each other.

3. JOINT CLUTTER MITIGATION IN THE TB-BASED MIMO RADAR

Let us consider the worst situation that most jamming signals resulted by terrain scatters or multipath propagations impinge on the receiver within the whole pre-determined SOI $\boldsymbol{\Omega}$ where the target is also located. This means that strong correlations among multipath jamming signals in fast-time domain may occur. To facilitate the mitigation, we assume that the jamming sources are motionless, i.e., no Doppler shift is introduced into the hot clutter signal for each terrain scatter or multipath propagation. In what follows, we first formulate the 3D STAP problem for the TB-based MIMO radar system followed by the rank analysis of the hot and cold clutter covariance matrices, then we present the proposed 3D STAP method.

3.1. 3D STAP Formulation and Clutter Rank Analysis

In 3D STAP, the number of Q (assume to be an odd number) fast-time taps (i.e., range bins) is employed in addition to the previously defined $LKN \times 1$ virtual space-(slow) time data vector. By stacking $\mathbf{y}(\zeta)$, $\zeta = \zeta_0 - \widetilde{Q}, \ldots, \zeta_0 + \widetilde{Q}$ in (5), the $QLKN \times 1$ virtual data vector $\mathbf{y}$ can be obtained as

$$\begin{aligned}\mathbf{y} &\triangleq \big[\mathbf{y}^T\big(\zeta_0-\widetilde{Q}\big),\ldots,\mathbf{y}^T\big(\zeta_0+\widetilde{Q}\big)\big]^T \qquad (6)\\ &= \mathbf{y}_{\mathrm{t}}+\mathbf{y}_c+\mathbf{y}_h+\tilde{\mathbf{z}} \qquad (7)\end{aligned}$$

where $\widetilde{Q} \triangleq (Q-1)/2$ and $\mathbf{y}_{\mathrm{t}}$, $\mathbf{y}_c$, $\mathbf{y}_h$, and $\tilde{\mathbf{z}}$ are formed using the same way as $\mathbf{y}$ in (6) with the same size $QLKN \times 1$.

Using (7), the target-free interference covariance matrix of the virtual data vector $\mathbf{y}$ is defined as

$$\mathbf{R_y} \triangleq \mathbb{E}\{\mathbf{y}\mathbf{y}^H\} = \mathbb{E}\{\mathbf{y}_c\mathbf{y}_c^H\} + \mathbb{E}\{\mathbf{y}_h\mathbf{y}_h^H\} + \mathbb{E}\{\tilde{\mathbf{z}}\tilde{\mathbf{z}}^H\} \triangleq \mathbf{R_c} + \mathbf{R_h} + \mathbf{R_{\tilde{z}}} \quad (8)$$

where $\mathbf{R_c}$, $\mathbf{R_h}$, and $\mathbf{R_{\tilde{z}}}$ stand for the covariance matrices of the cold clutter, the hot clutter, and the noise, respectively, and $\mathbb{E}\{\cdot\}$ is the expectation operator.

The objective of the 3D STAP is to find an adaptive filter (with a $QLKN \times 1$ weight vector $\mathbf{w}$) that maximizes the output SINR. This filter can be obtained by solving the following minimum variance distortionless response (MVDR) type optimization problem

$$\begin{aligned} \min_{\mathbf{w}} \quad & \mathbf{w}^H \mathbf{R_y} \mathbf{w} \\ \text{s.t.} \quad & \mathbf{w}^H \mathbf{s}_{\mathrm{t}}\big(\bar{Q}, f_s(\theta_{\mathrm{t}}), f_d(\theta_{\mathrm{t}})\big) = 1 \end{aligned} \quad (9)$$

where $f_s(\theta_{\mathrm{t}})$ and $f_d(\theta_{\mathrm{t}})$ are the spatial and the Doppler frequencies of the target, respectively, and $\mathbf{s}_{\mathrm{t}}\big(\bar{Q}, f_s(\theta_{\mathrm{t}}), f_d(\theta_{\mathrm{t}})\big)$ is the target steering vector which can be expressed as

$$\mathbf{s}_{\mathrm{t}}\big(\bar{Q}, f_s(\theta_{\mathrm{t}}), f_d(\theta_{\mathrm{t}})\big) \triangleq \mathbf{e}_{\bar{Q}} \otimes \mathbf{d}(\theta_{\mathrm{t}}) \otimes \mathbf{u}\big(\theta_{\mathrm{t}}, \bar{Q}\big) \otimes \mathbf{b}(\theta_{\mathrm{t}}) \quad (10)$$

with $\bar{Q} \triangleq (Q+1)/2$ and $\mathbf{e}_{\bar{Q}}$ being a $Q \times 1$ all-zero vector except the $\bar{Q}$th entry replaced by 1.

The MVDR problem (9) leads to the following solution [24]

$$\mathbf{w} = \frac{\mathbf{R_y^{-1}} \mathbf{s}_{\mathrm{t}}\big(\bar{Q}, f_s(\theta_{\mathrm{t}}), f_d(\theta_{\mathrm{t}})\big)}{\mathbf{s}_{\mathrm{t}}^H\big(\bar{Q}, f_s(\theta_{\mathrm{t}}), f_d(\theta_{\mathrm{t}})\big) \mathbf{R_y^{-1}} \mathbf{s}_{\mathrm{t}}\big(\bar{Q}, f_s(\theta_{\mathrm{t}}), f_d(\theta_{\mathrm{t}})\big)}. \quad (11)$$

Let us take the TB strategy that aims at approximating linear phase rotations among the K transmit beams for example, i.e., $\mathbf{C}^H \mathbf{a}(\theta_b) \simeq \mathbf{g}(\theta_b) \triangleq [e^{j\mu_1(f_s(\theta_b))}, \ldots, e^{j\mu_K(f_s(\theta_b))}]^T$, $b = 1, \ldots, B$ where $\mu_i(f_s(\theta_b))$, $i = 1, \ldots, K$ are uniform linear functions of the spatial frequency $f_s(\theta_b)$, and B is the number of angular grids used for approximating the SOI $\mathbf{\Omega}$.

The matrix $\mathbf{R_c}$ takes the form $\mathbf{R_c} = \mathrm{diag}\{\mathbf{R}_{\mathbf{c},-\bar{Q}}, \ldots, \mathbf{R}_{\mathbf{c},\bar{Q}}\}$ where $\mathrm{diag}\{\cdot\}$ stands for the diagonalization operation and $\mathbf{R}_{\mathbf{c},q}$, $q \in \{-\bar{Q}, \ldots, \bar{Q}\}$ is the $LKN \times LKN$ space-(slow) time cold clutter covariance matrix for the qth range bin whose rank is $r_0 \triangleq \lceil N + \rho(K-1) + \eta(L-1) \rceil$. Here ρ is the ratio between the synthesized transmit aperture (i.e., the one associated with $\mathbf{g}(\theta)$) and the receive one, η is the ratio between radar movement in one pulse and the neighbour receive antenna element space, and $\lceil \cdot \rceil$ is the ceiling function. Thus, the rank of $\mathbf{R_c}$ is $r_c \triangleq Q\lceil N + \rho(K-1) + \eta(L-1) \rceil$. Considering that hot clutter is not correlated to pulses and assuming that TB processing does not affect its wide stationarity, the matrix $\mathbf{R_h}$ takes the form $\mathbf{R_h} = \mathbf{R}_Q \otimes (\mathbf{I}_{LK} \otimes \mathbf{R}_N)$ where $\mathbf{R}_Q$ is a $Q \times Q$ fast-time Toeplitz cross-correlation matrix which is dependent on the bandwidth of jamming signal, and $\mathbf{R}_N$ is an $N \times N$ spatial covariance matrix of jamming multipath. Generally, $\mathbf{R_h}$ has a rank that is QLK times rank of $\mathbf{R}_N$, however, it contains $Q \times Q$ space-(slow) time diagonal blocks. The noise covariance matrix $\mathbf{R_{\tilde{z}}}$ takes the form $\mathbf{R_{\tilde{z}}} = \sigma_z^2 \widetilde{\mathbf{R}}_Q \otimes \mathbf{I}_{LKN}$ where $\widetilde{\mathbf{R}}_Q$ is a $Q \times Q$ fast-time cross-correlation matrix of noise resulted by range sidelobes.

Note that $\mathbf{R_h}$ is in general a function of the fast time t, and it differs for different pulses if motions of jamming sources are considered. Although 3D STAP is still effective, here we aim at presenting the potential of the TB-based MIMO radar in motionless hot clutter environment.

3.2. Proposed 3D STAP Method

Let us deal with the case when range sidelobes are well controlled or negligible[1] and no overlap occurs in fast-time sampling. Thus, $\mathbf{R_{\tilde{z}}}$ becomes an identity matrix of size $QLKN \times QLKN$, i.e., $\mathbf{R_{\tilde{z}}} = \sigma_z^2 \mathbf{I}_{QLKN}$. Let $\mathbf{R_{h\tilde{z}}} \triangleq \mathbf{R_h} + \mathbf{R_{\tilde{z}}}$, then $\mathbf{R_{h\tilde{z}}}$ can be expressed as

$$\mathbf{R_{h\tilde{z}}} = \mathbf{R}_Q \otimes \big(\mathbf{I}_{LK} \otimes \widetilde{\mathbf{R}}_N\big) - \sigma_z^2 \bar{\mathbf{R}}_Q \otimes \mathbf{I}_{LKN} \quad (12)$$

where $\widetilde{\mathbf{R}}_N \triangleq \mathbf{R}_N + \sigma_z^2 \mathbf{I}_N$, and $\bar{\mathbf{R}}_Q$ is identical to $\mathbf{R}_Q$ except for the main diagonal elements which are replaced by zeros. Block diagonal property of $\mathbf{R_h}$ is preserved in $\mathbf{R_{h\tilde{z}}}$.

Since the matrices $\mathbf{R}_{\mathbf{c},q}$, $q = -\bar{Q}, \ldots, \bar{Q}$ share the same clutter rank r_0, there exists an $r_0 \times r_0$ matrix $\mathbf{\Lambda}_q$ for the qth sub clutter covariance matrix which satisfies $\mathbf{R}_{\mathbf{c},q} \simeq \mathbf{S}_q \mathbf{\Lambda}_q \mathbf{S}_q^H$. The quality of this approximation depends on the ratio $\gamma = \sum_{k=1}^{r_0} \lambda_k^q / \sum_{k=1}^{LKN} \lambda_k^q$ where λ_k^q is the kth eigenvalue of $\mathbf{R}_{\mathbf{c},q}$ whose eigenvalues are ordered in decreasing manner. Let us define the cold clutter subspace as $\mathbf{S_c} \triangleq \mathrm{diag}\{\mathbf{S}_{-\bar{Q}}, \ldots, \mathbf{S}_{\bar{Q}}\}$, then the whole cold clutter matrix $\mathbf{R_c}$ can be expressed as $\mathbf{R_c} \simeq \mathbf{S_c} \mathbf{\Lambda} \mathbf{S_c}^H$ where $\mathbf{\Lambda}$ is an $r_c \times r_c$ matrix. The overall clutter covariance matrix $\mathbf{R_y}$ can then be re-expressed as

$$\mathbf{R_y} \simeq \mathbf{R_{h\tilde{z}}} + \mathbf{S_c} \mathbf{\Lambda} \mathbf{S_c}^H. \quad (13)$$

The expression (13) leads to the following inversion

$$\mathbf{R_y}^{-1} \simeq \mathbf{R_{h\tilde{z}}}^{-1} - \mathbf{R_{h\tilde{z}}}^{-1} \mathbf{S_c} \big(\mathbf{\Lambda}^{-1} + \mathbf{S_c}^H \mathbf{R_{h\tilde{z}}}^{-1} \mathbf{S_c}\big)^{-1} \mathbf{S_c}^H \mathbf{R_{h\tilde{z}}}^{-1} \quad (14)$$

where the matrix inversion lemma is used in the derivation, and the inverse of $\mathbf{R_{h\tilde{z}}}$ can be achieved by the following approximation

$$\mathbf{R_{h\tilde{z}}}^{-1} \simeq \sum_{k=0}^{\kappa} \sigma_z^{2k} \Big(\mathbf{R}_Q^{-1} \otimes \mathbf{I}_{LK} \otimes \widetilde{\mathbf{R}}_N^{-1}\Big) \times \Big(\mathbf{R}_Q^{-1} \bar{\mathbf{R}}_Q\Big)^k \otimes \mathbf{I}_{LK} \otimes \widetilde{\mathbf{R}}_N^{-k} \quad (15)$$

with κ being the order of Taylor expansion for the inverse of (12), if the corresponding convergence condition is satisfied. It only requires calculating the inverse of $\mathbf{R}_Q$ and $\widetilde{\mathbf{R}}_N$.

[1] This can be achieved by employing waveforms with good correlation properties or by artificially controlling the sidelobe levels within a certain range of fast time. The corresponding range-Doppler "clear region" is between that of the PA and traditional MIMO radar cases, depending on the number of the synthesized transmit beams K [13], [23].

Using (13) and also (8), the matrix $\mathbf{\Lambda}$ can be obtained as

$$\mathbf{\Lambda} = \mathbf{R}_{\tilde{\mathbf{y}}} - \mathbf{U}^H \mathbf{R}_{\mathbf{h}\tilde{\mathbf{z}}} \mathbf{U} \tag{16}$$

where $\mathbf{U} \triangleq \operatorname{diag}\{\mathbf{S}_{-\bar{Q}}(\mathbf{S}^H_{-\bar{Q}}\mathbf{S}_{-\bar{Q}})^{-1}, \ldots, \mathbf{S}_{\bar{Q}}(\mathbf{S}^H_{\bar{Q}}\mathbf{S}_{\bar{Q}})^{-1}\}$ and $\mathbf{R}_{\tilde{\mathbf{y}}} \triangleq \mathbb{E}\{\tilde{\mathbf{y}}\tilde{\mathbf{y}}^H\}$ with $\tilde{\mathbf{y}} \triangleq \mathbf{U}^H\mathbf{y}$.

One way to obtain the qth clutter subspace $\mathbf{S}_q$ is to span using N_c space-(slow) time antenna array steering vectors of the qth range bin. Hence, the 3D STAP solution can be achieved by substituting (14) into (11). In practice, $\widetilde{\mathbf{R}}_N$ is estimated using the $N \times 1$ target and clutter free signals at the receiver by switching radar to the passive receive mode, $\mathbf{R}_Q$ is estimated based on fast-time samples, and $\mathbf{R}_{\tilde{\mathbf{y}}}$ is estimated using the transformed 3D samples $\tilde{\mathbf{y}}$.

4. SIMULATION RESULTS

We use uniform linear arrays of half wavelength spaced $M = 16$ transmit and $N = 5$ receive antenna elements. The total transmit energy is set to be $E = M$. We select $\mathbf{\Omega} = [10°, 25°]$ as the SOI and $10°$ width as the transition band for the TB-based MIMO radar. This leads to a minimum selection of $K = 4$ waveforms according to the procedure in [8]. The radar platform is assumed to be moving with a velocity of 125 m/s, and there are $L = 5$ pulses in one CPI with pulse repetition frequency being $f_r = 500$ Hz. The target is located at $\theta_t = 16°$ and has a relative Doppler $f_d = 0.14$. We assume that 100 diffuse scatters are uniformly distributed within $\mathbf{\Omega}$ for each range bin. The hot and cold clutter-to-noise ratios are both set to be 50 dB, and the SNR (before processing) is 0 dB. We select $Q = 3$ range bins due to high correlation of multipath jamming, and the target is located at the middle one.

In the first example, we show the high-resolution clutter spectra of the ROI (see Fig. 1). The spectra is defined as $P(f_s, f_d) \triangleq \left(\mathbf{s}^H(f_s, f_d)\mathbf{R}_{\mathbf{y}}^{-1}\mathbf{s}(f_s, f_d)\right)^{-1}$ [22] where $\mathbf{s}(f_s, f_d)$ is the space-(slow) time antenna array steering vector achieved from (10) by enforcing $Q = 1$. Fig. 1(a) shows the clutter spectra when only cold clutter is present. It can be seen that the cold clutter ridge concentrates on the region of SOI, meaning that more cold clutter energy is focused because of the TB strategy. The off-ridge area is clean. Fig. 1(b) shows the case when hot clutter is also present. It can be seen that the region of SOI ($f_s \in [0.09, 0.21]$) is completely contaminated by the hot clutter, and all the Doppler frequencies of this region are occupied. Moreover, the ridge of the cold clutter spreads at a certain extent. This means that if potential target is present in this area, it is submerged in harsh hybrid clutter.

In the second example, we evaluate the output SINR performance of clutter mitigation (see Fig. 2). The SINR is defined as SINR $= \sigma_\alpha^2 E \mathbf{w}^H \mathbf{s}_t \mathbf{s}_t^H \mathbf{w} / K \mathbf{w}^H \mathbf{R}_{\mathbf{y}} \mathbf{w}$. We employ 10 samples to estimate $\mathbf{R}_Q$ and $\widetilde{\mathbf{R}}_N$, and 30 samples to estimate $\mathbf{R}_{\tilde{\mathbf{y}}}$ when evaluating the SINR performance of the TB-based MIMO radar with spheroidal sequences-based and convex optimization-based TB designs (see [8]) using the proposed 3D STAP method. The optimal output SINR associated with the former TB design is about 1 dB better than that associated with the latter one. It can be seen that the proposed method shows good clutter mitigation performance for both TB designs. The convex optimization-based design gives better (about 2 dB) SINR than the spheroidal sequences-based one, meaning that proper TB design is prone to achieve good clutter mitigation performance. The optimal SINR of the TB-based MIMO radar is about 6$\sim$7 dB higher than that of the the traditional MIMO radar because of the energy focusing in the TB designs.

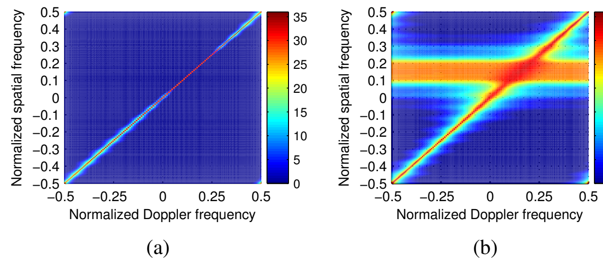

Fig. 1. Clutter spectra of the TB-based MIMO radar.

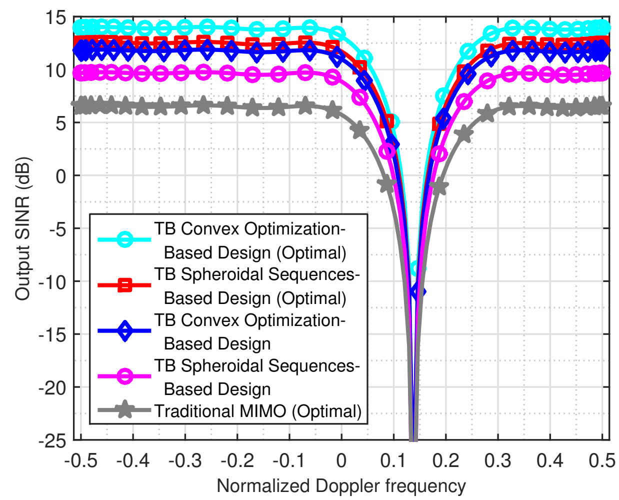

Fig. 2. SINR performance versus Doppler frequencies.

5. CONCLUSIONS

We have considered the problem of joint hot and cold clutter mitigation in the context of the TB-based MIMO radar which has not been studied before. The energy of the cold clutter is shown to be focused in this type of radar configuration, while the hot clutter contaminates the whole SOI. 3D STAP technique has been employed to mitigate the hybrid clutter. We have formulated the STAP problem and analyzed the rank of the hot and cold clutter covariance matrices. By utilizing the low-rank and block diagonal properties of the clutter covariance matrices, a new 3D STAP method with lower computational complexity has been developed. It has been also shown that the TB-based MIMO radar enables superior output SINR to that of its traditional MIMO radar counterpart.

6. REFERENCES

[1] J. Li and P. Stoica, "MIMO radar with colocated antennas," *IEEE Signal Process. Mag.*, vol. 24, no. 5, pp. 106–114, Sep. 2007.

[2] A. M. Haimovich, R. S. Blum, and L. J. Cimini, "MIMO radar with widely separated antennas," *IEEE Signal Process. Mag.*, vol. 24, no. 1, pp. 116–129, Jan. 2008.

[3] E. Fishler, A. Haimovich, R. S. Blum, L. Cimini, D. Chizhik, and R. Valenzuela, "Spatial diversity in radars—Models and detection performance," *IEEE Trans. Signal Process.*, vol. 54, no. 3, pp. 823–838, Mar. 2006.

[4] C.-Y. Chen and P. P. Vaidyanathan, "MIMO radar space-time adaptive processing using prolate spheroidal waveform functions," *IEEE Trans. Signal Process.*, vol. 56, no. 2, pp. 623–635, Feb. 2008.

[5] D. R. Fuhrmann and G. San Antonio, "Transmit bemforming for MIMO radar systems using signal cross-correlation," *IEEE Trans. Aerosp. Electron. Syst.*, vol. 44, no. 1, pp. 171–186, Jan. 2008.

[6] P. Stoica, J. Li, and Y. Xie, "On probing signal design for MIMO radar," *IEEE Trans. Signal Process.*, vol. 55, no. 8, pp. 4151–4161, Aug. 2007.

[7] A. Hassanien and S. A. Vorobyov, "Phased-MIMO radar: A tradeoff between phased-array and MIMO radars," *IEEE Trans. Signal Process.*, vol. 58, no. 6, pp. 3137–3151, Jun. 2010.

[8] A. Hassanien and S. A. Vorobyov, "Transmit energy focusing for DOA estimation in MIMO radar with colocated antennas," *IEEE Trans. Signal Process.*, vol. 59, no. 6, pp. 2669–2682, Jun. 2011.

[9] B. Friedlander, "On transmit beamforming for MIMO radar," *IEEE Trans. Aerosp. Electron. Syst.*, vol. 48, no. 4, pp. 3376–3388, Oct. 2012.

[10] A. Khabbazibasmenj, A. Hassanien, S. A. Vorobyov, and M. W. Morency, "Efficient transmit beamspace design for search-free based DOA estimation in MIMO radar," *IEEE Trans. Signal Process.*, vol. 62, no. 6, pp. 1490–1500, Mar. 2014.

[11] V. F. Mecca, D. Ramakrishnan, and J. L. Krolik, "MIMO radar space-time adaptive processing for multipath clutter mitigation," in *Proc. IEEE Sensor Array Multichannel Signal Process. Workshop*, Waltham, MA, Jul. 2006, pp. 249–253.

[12] Q. He, N. H. Lehmann, R. S. Blum, and A. M. Haimovich, "MIMO radar moving target detection in homogeneous clutter," *IEEE Trans. Aerosp. Electron. Syst.*, vol. 46, no. 3, pp. 1290–1301, Jul. 2010.

[13] Y. Li, S. A. Vorobyov, and V. Koivunen, "Generalized ambiguity function for the MIMO radar with correlated waveforms," in *Proc. IEEE Int. Conf. Acoust., Speech, Signal Process. (ICASSP)*, Florence, Italy, May 2014, pp. 5322–5326.

[14] Y. Li, S. A. Vorobyov, and A. Hassanien, "MIMO radar capability on powerful jammers suppression," in *Proc. IEEE Int. Conf. Acoust., Speech, Signal Process. (ICASSP)*, Florence, Italy, May 2014, pp. 5277–5281.

[15] Y. Li, S. A. Vorobyov, and A. Hassanien, "Robust beamforming for jammers suppression in MIMO radar," in *Proc. IEEE Radar Conf.*, Cincinnati, OH, May 2014, pp. 0629–0634.

[16] L. J. Griffiths, "Linear constraints in hot clutter cancellation," in *Proc. IEEE Int. Conf. Acoust., Speech, Signal Process. (ICASSP)*, Atlanta, GA, May 1996, pp. 1181–1184.

[17] J. Ward, "Space-time adaptive processing for airborne radar," MIT Lincoln Lab., Lexington Massachusetts, MA, Technical Rep. 1015, Dec. 1994.

[18] R. L. Fante and J. A. Torres, "Cancellation of dissuse jammer multipath by an airborne adaptive radar," *IEEE Trans. Aerosp. Electron. Syst.*, vol. 31, no. 2, pp. 805–820, Apr. 1995.

[19] Y. I. Abramovich, N. K. Spencer, S. J. Anderson, and A. Y. Gorokhov, "Stochastic-constraints method in nonstationary hot-clutter cancellation—Part I: Fundamentals and supervised training applications," *IEEE Trans. Aerosp. Electron. Syst.*, vol. 34, no. 4, pp. 1271–1291, Oct. 1998.

[20] P. M. Techau, J. R. Guerci, T. H. Slocumb, and L. J. Griffiths, "Performance bounds for hot and cold clutter mitigation," *IEEE Trans. Aerosp. Electron. Syst.*, vol. 35, no. 4, pp. 1235–1265, Oct. 1999.

[21] W. L. Melvin, "A STAP overview," *IEEE Trans. Aerosp. Electron. Syst.*, vol. 19, no. 1, pp. 19–35, Jan. 2004.

[22] R. Klemm, *Principles of space-time adaptive processing*, 3rd ed. London, United Kingdom: The Institution of Electrical Engineering and Technology, 2006.

[23] Y. Li, S. A. Vorobyov, and V. Koivunen, "Ambiguity function of the transmit beamspace-based MIMO radar," *IEEE Trans. Signal Process.*, revised, Jan. 2015.

[24] H. L. Van Trees, *Optimum array processing*. New York: Wiley, 2002.